Electronic effects of ion mobility in semiconductors: Mixed electronic–ionic behavior and device creation in Si:Li

Leonid Chernyak,[a] Vera Lyakhovitskaya,[b] and Shachar Richter[b]
Department of Materials and Interfaces, Weizmann Institute of Science, Rehovot 76100, Israel

Abram Jakubowicz
IBM Research Division, Zürich Laboratory, Rüschlikon, Switzerland

Yishay Manassen
Department of Chemical Physics, Weizmann Institute of Science, Rehovot 76100, Israel

Sidney R. Cohen
Department of Chemical Services, Weizmann Institute of Science, Rehovot 76100, Israel

David Cahen[c]
Department of Materials and Interfaces, Weizmann Institute of Science, Rehovot 76100, Israel

(Received 3 November 1995; accepted for publication 22 May 1996)

Micrometer-sized homojunction structures can be formed by applying strong electric pulses, at ambient temperatures, to Li-doped, floating zone n-Si. Two such junctions, arranged back to back, act as a transistor, as evidenced by electron-beam-induced current and current–voltage measurements. The structures are created during a time ranging from ~100 ms to a few seconds, depending on the size of the structure. The phenomenon is similar to what was observed earlier in $CuInSe_2$ and was explained there by thermally assisted electromigration of Cu. In the case of Si doped with Li we can use secondary-ion-mass spectrometry to detect the redistribution of Li after electric-field application. Such a redistribution is indeed found and corresponds to an n^+-p-n structure with the p region extending at least ~20 μm into the bulk of Si. Structures created in Si doped with Li in this way are stable for at least 13 months after their creation. We ascribe this to the large difference between Li diffusivity at the local temperature that is reached during structure formation (~400 °C; 10^{-8} cm^2/s) and at room temperature (~10^{-15} cm^2/s). © *1996 American Institute of Physics.* [S0021-8979(96)01517-4]

I. INTRODUCTION

Li is known to be a fast-diffusing impurity in Si at temperatures of 400 °C and above.[1] It is electrically active as donor and is mainly located in the interstitial lattice sites of the diamond cubic lattice of this semiconductor. Extensive investigations on Li doping of Si and Ge were performed about 30–40 years ago.[1–4] The p-n junction technique was used in Ref. 1 to investigate the dependence of Li ion mobility on temperature. The possibility of using Li donors to create a compensated (i-intrinsic) region in Si was demonstrated and explained in Ref. 2. There it was shown that a p-i-n structure with an extended i region could be created when a p-n junction, formed in p-Si by Li in-diffusion, was reverse biased for several hours, at 50–125 °C. This property of Li ions is used to fabricate p-i-n Si detectors.[4]

On the basis of these properties of Li in Si and of our earlier findings that stable, nonequilibrium doping profiles form in chalcogenide semiconductors after applying an electric (E) field to them, we searched for similar phenomena in Li-doped Si (Si:Li). In the case of originally electrically homogeneous $CuInSe_2$, $(Cu,Ag)InSe_2$, or (Hg,Cd)Te crystals, local application of external E fields of up to 1 MV/cm resulted in the creation of ~100-μm-sized diode- and transistorlike structures in the bulk of these semiconductors.[5–7] We explained this behavior in terms of temperature-assisted electromigration of mobile native Cu, Ag, or Hg ions.[5–8] Even though the evidence for thermally assisted electromigration in these chalcogenides is strong, in all cases it is indirect, pending the outcome of ongoing radioactive tracer experiments. One of the attractive features of working with foreign, rather than native, dopants is that direct evidence can be obtained from secondary-ion-mass spectrometry (SIMS).

Here we show that results similar to the ones obtained for chalcogenide semiconductor $(Cu,Ag)InSe_2$ can be obtained for Si which was originally homogeneously doped with Li. Transistorlike structures were created in $(Cu,Ag)InSe_2$ by E-field application and results of capacitance–voltage ($C-V$), current–voltage ($I-V$), and electroluminescence (EL) measurements on these structures were reported.[5,7] Early results for Si:Li appeared in a preliminary communication.[9]

The outline of this article is as follows: Section II describes the materials used, experimental setups and techniques involved in the investigation. Section III starts with the presentation of the basic experiment, E-field-induced transistor structure creation in Si:Li. SIMS measurements performed on these structures are reported afterwards. These measurements suggest conductivity-type conversion. This was proven by scanning tunneling microscope (STM) spectroscopy and contact $I-V$ measurements. Results of the in-

[a]Present address: Dept. of Electrical Engineering, Colorado State University, Ft. Collins, CO 80521.
[b]Also with: Dept. of Chemical Physics.
[c]Author to whom correspondence should be addressed; Electronic mail: cscahenl@weizmann.weizmann.ac.il

Downloaded¬23¬Oct¬2002¬to¬132.72.138.3.¬Redistribution¬subject¬to¬AIP¬license¬or¬copyright,¬see¬http://ojps.aip.org/japo/japcr.jsp

vestigation of the kinetics of structure creation, of the temperature during this process, and of investigations of Si:Li near equilibrium follow. Experimental results that shed light on structure stability and device action and results of numerical simulations of electromigration of Li in Si are given at the end of this section. All these results are discussed in Sec. IV, which starts with estimating the electric field, something that is needed to understand the initiation of the process. Li–B pairing is then considered to allow a discussion of the evolution and of the limitations of the process of fast structure creation. Based on these discussions we present a coherent, qualitative model for the phenomenon of E-field-induced structure creation and compare the Si:Li and $CuInSe_2$ systems. Conclusions are summarized in Sec. V.

II. EXPERIMENT

Samples (0.75 mm thick) were taken from (111)-oriented, floating zone p-Si wafers (ρ=10 or 0.25 Ω cm). Such wafers have significantly higher Li ion mobility than Czochralski-grown ones because of the higher oxygen content of the latter leading to formation of Li–O complexes.[10] We doped the wafers homogeneously with Li, using a 30% Li dispersion in mineral oil. Both sides of the samples were covered, in Ar atmosphere, by the Li dispersion. The samples were then placed in a ceramic container and dried at 300–400 °C for 15 min in an Ar or N_2 atmosphere. They were then sealed in a quartz ampoule, evacuated under a pressure of 10^{-4} Torr, and annealed at temperatures ranging from 300 to 600 °C. This leads to type conversion of the samples from p to n. The electrical properties of the samples after doping were checked by four-probe resistivity and Hall measurements. These results, as well as the regimes of doping, are presented in Table I.

TABLE I. Electrical properties of the samples after doping.[a]

Sample	Majority carrier concentration (cm^{-3})	Specific resistance (Ω cm)	Mobility of carriers (cm^2/V s)	Doping regimes conditions for device creation
A	1.1×10^{15}	9	1260	Annealing at 300 °C for 3 h V=100 V I up to 15 mA
B	1.3×10^{16}	3.5	150	Annealing at 370 °C for 17 h V=150–200 V I up to 15 mA
C	4×10^{18}	0.01	120	Annealing at 500 °C for 16 h V=130 V I up to 15 mA
D	2.2×10^{17}	0.04	710	Annealing 380 °C for 17 h V=120 V (dc) I up to ~12 mA, or V=180 V I up to 15 mA

[a]Periodic, reverse bias voltage was used for all the samples listed in Table I, except for sample D to which both dc and periodic voltages were applied. The boron acceptor concentration in the samples was $\sim2\times10^{15}$ cm^{-3}, except for sample D, in which it was $\sim6.5\times10^{16}$ cm^{-3}.

Most experiments on structure creation in Si:Li were performed *in situ* in a Philips 515 scanning electron microscope (SEM). A tungsten needle with an average tip diameter of 10 μm was adjusted in the vacuum chamber of this microscope to be used as an electrode for voltage application to the samples. The X-Y-Z manipulator of the SEM sample holder was used to adjust the sample to the needle and to make contact to a predetermined spot on the top surface of Si. Such a contact was found to be rectifying (Schottky barrier). Ohmic back contact was made to the bottom surface of the sample by connecting it to the sample stage using Ag paint. This configuration is shown in Fig. 1(a).

External voltage was applied to the samples using a custom-made power supply which generates a trapezoidal or triangular voltage [Fig. 1(b)]. The trapezoidal high voltage, ranging from 0 to 500 V, is used to modify the local properties of the samples. The sawtoothlike low voltage (from −5 to 5 V) follows the high voltage and serves for the low-voltage I–V measurements. In-house software allowed recording of low- and high-voltage I–V curves. A microheater, adjusted inside the vacuum chamber of the SEM, allows heating of the samples up to 350 °C during voltage application.

The time course of structure creation could be followed by incorporating a digital, memory oscilloscope (Le Croy 9310M) into the circuit used for measuring the high-voltage I–V characteristics. In this way the current–time characteristics were recorded when the current exceeded a certain preset value. Preliminary measurements served to determine the

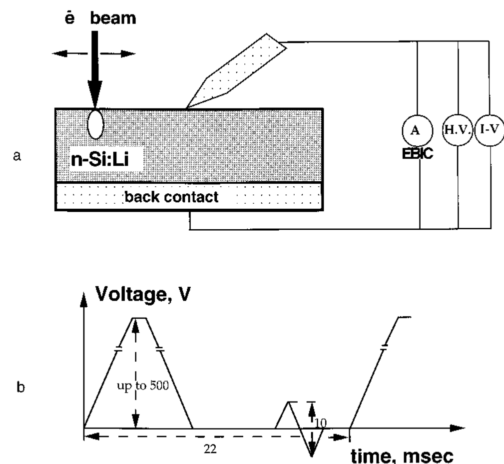

FIG. 1. (a) Scheme of experimental setup in the scanning electron microscope. One surface of the sample is used as a back contact. Any point of the other surface can be contacted using the X-Y-Z micropositioning capability of the SEM. As the electron beam of the SEM scans across the top surface, current is induced by the electron beam and is measured using the SEM. A mixed high- and low-voltage signal is applied to a sample to change locally its electrical properties (high voltage) and to follow these changes (low voltage). (b) Shape and time dependence of the applied external voltage, showing the trapezoidal high voltage (adjustable up to 500 V) and sawtooth-like low voltage (adjustable up/down to ±5 V). The plot corresponds to 45 Hz frequency. The frequency of the applied voltage can be changed from 7 to 45 Hz.

Downloaded¬23¬Oct¬2002¬to¬132.72.138.3.¬Redistribution¬subject¬to¬AIP¬license¬or¬copyright,¬see¬http://ojps.aip.org/japo/japcr.jsp

steady-state current value, and a slightly higher current value was used as the preset value.

Changes in the local electrical properties of samples as a result of E-field application were detected using electron-beam-induced current (EBIC) in the SEM. Details of this technique can be found elsewhere.[11] By connecting the current amplifier and the control output of the SEM scanning coil to a computer, single EBIC line scans were recorded digitally.

Transistor action of the device structures that were created was demonstrated in the two-terminal ''phototransistor'' mode. $I-V$ measurements were performed *in situ* in the SEM. The top and bottom contacts which served for structure creation were used as emitter and collector. Mostly the electron beam of the SEM was used instead of a photon beam. The electron-beam current, induced in the semiconductor, was measured using a digital nanoammeter. Current through the structure was recorded as a function of the voltage applied between emitter and collector for different values of the electron-beam current. A Tektronix curve tracer served to record transistor $I-V$ curves.

Some $I-V$ measurements were performed inside a controlled atmosphere multiple micromanipulator (MMR Industries), evacuated to a pressure of 20 mTorr, using a He–Ne laser ($\lambda=632.8$ nm) as a photon beam. The laser beam was focused by a collection lens down to ~ 5 μm. This beam entered the micromanipulator through a sapphire window. By displacing the focusing lens in the plane perpendicular to the incident laser beam it was possible to scan the surface of the sample. The intensity of the radiation was changed by neutral density filters and was measured using a radiant power meter.

Ambient STM was used to distinguish between n- and p-type Si as described, for example, in Ref. 12. We used a Topometrix TMX2010 Discoverer STM to perform $I_{\text{tunnel}}-V$ spectroscopy with a 90%/10% Pt/Ir tip at different points above the sample surface. By varying the position of the tip over an area under which a device structure had been created, the local electrical properties were tested. The current/voltage setpoint (1 nA at -2 V tip bias) was used to fix the tip–surface distance at each measurement point.

Secondary ion mass spectrometry (SIMS) measurements were performed, before and after E-field application. A CAMECA spectrometer (at the Solid State Institute of the Technion, Haifa), using a 12 keV O_2^+ beam, was used. An 8×8 μm^2 square area was analyzed during the measurements. Additional details about SIMS can be found, for example, in Ref. 13.

III. RESULTS

The basic experimental observation is that transistorlike structures form when a -100 to -200 V (periodic or dc) reverse bias is applied to a needle–n-Si:Li semiconductor contact [Fig. 1(a)]. The structure forms around this contact. Structure creation takes place when a certain minimal voltage is exceeded and is detected by an abrupt increase of current. The current increases from a steady-state value of

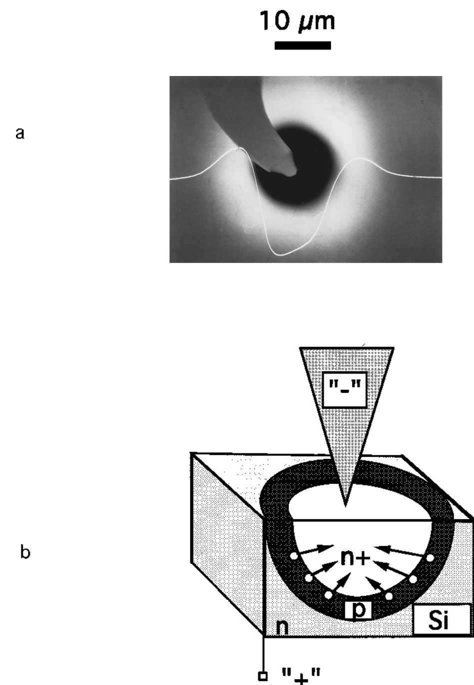

FIG. 2. (a) EBIC contrast and superimposed line scan of an electric-field-induced structure, created in sample A. Experimental conditions for EBIC: accelerating voltage 30 kV; electron-beam spot size 500 nm. Black EBIC contrast (negative line scan) corresponds to n^+-p junction (b); white EBIC contrast (positive line scan) corresponds to p-n junction. (b) Schematic explanation of structure creation. Arrows represent the direction of Li electromigration.

$\sim$3–7 to $\sim$15 mA (without any change in applied periodic voltage) over a time period varying from 100 ms to 1–2 min (see discussion below).

In this way a transistorlike structure was created in sample B by applying a reverse bias *in situ* in the SEM. Figure 2(a) shows an EBIC contrast picture and line scan from this structure. Figure 2(b) shows schematically how redistribution of Li in Si can lead to such structure creation. Li^+ ions are collected under the negatively charged W needle, due to Coulombic electromigration. Such migration can occur in the high electric field (up to 10^6 V/cm) that exists in the space-charge region of the reverse-biased Schottky barrier created between the W needle and the top surface of the semiconductor. The region where the Li ions are collected becomes n^+, while the region that is depleted of Li ions can type convert to p type (see discussion below). The bulk of the material, which is unaffected by the E field, remains n type (Table I).

Based on, and in analogy to, previous results on $CuInSe_2$ we ascribe this phenomenon to thermally assisted electromigration of mobile Li ions in the E field. In this case, however, we are able to present direct evidence for Li redistribution in Si:Li, something that was not possible for Cu in $CuInSe_2$.

A. SIMS investigation of Li electromigration

SIMS measurements were performed through a structure of the type shown in Fig. 2(b) [see also Fig. 8(b)], as well as under a nonbiased spot [Fig. 3(a)]. The bulk of the sample is homogeneously doped with Li at concentrations between

Downloaded¬23¬Oct¬2002¬to¬132.72.138.3.¬Redistribution¬subject¬to¬AIP¬license¬or¬copyright,¬see¬http://ojps.aip.org/japo/japcr.jsp

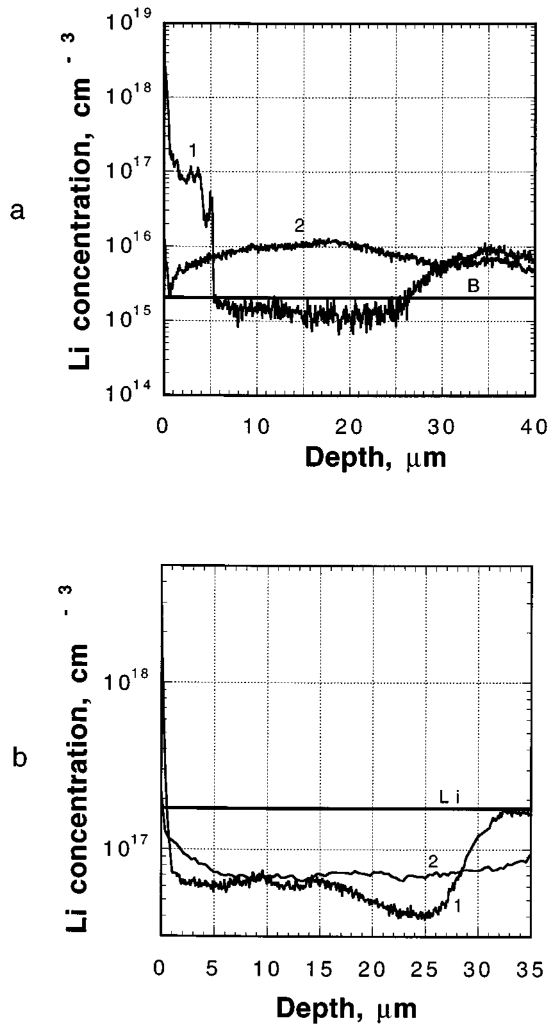

FIG. 3. Li and B SIMS profiles before and after E-field application to Si:Li samples. (a) SIMS measurements on sample B: 1: Li profile through the center of transistorlike structure [Fig. 8(b)]; 2: Li profile through a point which was not affected by the electric field. The straight line represents the level of acceptors (boron) in this sample. (b) SIMS measurements on sample D: 1: Li profile through the center of transistorlike structure; 2: B (acceptor) profile through a point not affected by E field. The straight line represents the level of equilibrium Li distribution.

$\sim 5\times 10^{15}$ and $\sim 1\times 10^{16}$ cm^{-3}, as shown by profile 2 in Fig. 3(a). In that profile the abrupt decrease of Li concentration close to the surface is very likely explained by the high etching rate of ~ 0.5 μm/min, used during the measurements. Profile 1 of Fig. 3(a) was obtained by measuring through the center of a transistor structure [Fig. 8(b)]. The level of boron acceptors is shown in this figure as a straight line.

Results similar to those presented in Fig. 3(a) were obtained for sample D treated in a manner similar to that described for sample B. Profile 1 of Fig. 3(b) shows the redistribution of Li under the point of voltage application. Profile 2 of Fig. 3(b) presents the concentration of boron in the sample (it was originally p type; Sec. II). The concentration and distribution of Li before voltage application is shown as a straight line in Fig. 3(b).

SIMS thus provides direct evidence for Coulombic electromigration of Li ions under the influence of an E field. This can be understood from results for $CuInSe_2$, shown in Fig. 3 of Ref. 5. Those show that the planar EBIC profile reflects the cross-sectional one (i.e., a hemispherical region, centered around the contact, is affected by the E field). Therefore, the SIMS depth profile can be correlated with the planar EBIC profile [Fig. 2(a)]. Using this correlation we conclude that the E-field-induced changes of conductivity type in originally electrically homogeneous n-type Si:Li are due to Li electromigration. The SIMS profiles further suggest that actual conductivity-type conversion from n to p takes place, as suggested in Fig. 2(b).

B. Conductivity type conversion

The Li concentration profile 1 of Fig. 3(a), and profile 1 of Fig. 3(b) fall below the equilibrium concentration of Li [see profile 2 of Fig. 3(a) and level of equilibrium Li concentration indicated in Fig. 3(b)] and slightly below the boron level for samples B and D. This suffices for type conversion from n to p. SIMS shows for both samples that an extended region (~ 20 μm) over which the material may be type converted, has been created. Assuming 100% ionization, we estimate the average majority carrier concentration in the p region that has been created to be $\sim 1\times 10^{15}$ and $\sim 2\times 10^{16}$ cm^{-3} for samples B and D, respectively. The accuracy of these SIMS measurements is $\sim 30\%$. Therefore, the concentration of Li in the Li-deficient region may, in fact, be higher than that of boron, in which case there will be no conversion from n to p type; however, STM spectroscopy and $I-V$ measurements support the conclusion that type conversion occurs.

1. STM spectroscopy

Type conversion from n to p and then back to n was observed when a STM tip was scanned across the structures created in samples B and D. Typical $I_{tunnel}-V$ curves are presented in Figs. 4(a)–4(c) (sample B). Figure 4(a) is obtained when the bulk, n-type region outside the transistor structure is probed. The bulk material is known to show n-type behavior from Hall and EBIC measurements. An additional indication for this is found in the slight asymmetry of the $I_{tunnel}-V$ curve presented in Fig. 4(a): for an n-type sample a higher positive than negative tip voltage has to be applied to get a tunneling current. Figure 4(b) presents the p-type region of the n^+-p-n structure [Fig. 2(b)]. The asymmetry of the $I-V$ curve is here much clearer, and inverted with respect to that of Fig. 4(a). Figure 4(c) shows that the conductivity type changes back to n when the spectroscopy is measured in the center of the transistor structure. This $I_{tunnel}-V$ curve is extremely asymmetrical, as compared to Fig. 4(a), thus providing evidence for the creation of an n^+ region. The appearance of tunneling current at voltages corresponding to energies that are higher than the width of the forbidden gap of Si (and SiO_2)[14] can be explained by tip-induced band bending.[15]

Similar results were obtained on sample B by contacting the n^+, p, and n regions of this structure directly by W probes (~ 2 μm tip diameter) in the controlled atmosphere

Downloaded¬23¬Oct¬2002¬to¬132.72.138.3.¬Redistribution¬subject¬to¬AIP¬license¬or¬copyright,¬see¬http://ojps.aip.org/japo/japcr.jsp

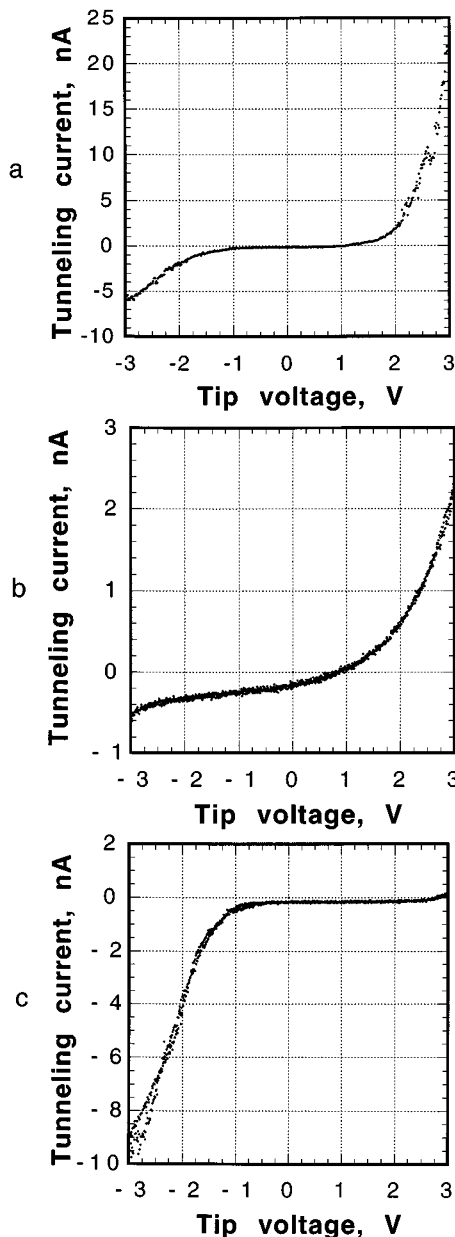

FIG. 4. STM $I-V$ spectroscopy on various parts of a transistor structure created in sample B: (a) $I-V$ curve taken with the tip above n region [Fig. 2(b)]; (b) $I-V$ curve taken with the tip above p region [Fig. 2(b)]; (c) $I-V$ curve taken with the tip above n^+ region [Fig. 2(b)].

micromanipulator (Fig. 5). The measurements were started in the center of the structure (n^+ region) and were directed toward the n region [Fig. 5(f)]. The $I-V$ curves corresponding to these measurements are presented in Figs. 5(a)–5(f). We see a clear transition from the $I-V$ curve corresponding to a Schottky barrier on n-type Si [Fig. 5(a)] to that of a Schottky barrier on p-type Si [Fig. 5(d)], and then back to n-type Si [Fig. 5(f)]. Therefore, an n^+-p-n transistor structure is created during external voltage (electric field) application. Results on contacting $I-V$ curve measurements across a transistor structure created in (Cu,Ag)$InSe_2$ are reported in Ref. 16. Insight into the process of structure creation can be obtained from studies of the kinetics of the process.

C. Kinetics of structure creation

Structure creation can be separated into two stages:

(1) fast Li electromigration, lasting ~100 ms, and
(2) slower Li electromigration, lasting dozens of seconds.

This latter stage is, probably, similar to normal Li electromigration in Si.[4]

Figures 6(a) and 6(b) present the low- and high-voltage $I-V$ curves, respectively, from the W-needle–semiconductor Schottky barrier on sample A just before the process of transistor structure creation starts. When the applied high voltage is slightly increased above the maximum value seen in Fig. 6(b), an abrupt increase of current through the semiconductor is observed [Fig. 6(d)]. The hysteresis in the high-voltage $I-V$ curve [Fig. 6(d)] is attributed to the displacement of Li ions (see also Ref. 7). The low-voltage $I-V$ curve [Fig. 6(c)], recorded immediately afterwards [see the voltage–time dependence presented in Fig. 1(b)] was also changed. After ~100 ms the high-voltage $I-V$ curve reverts to the initial situation seen in Fig. 6(f). The subsequent low-voltage $I-V$ curve [Fig. 6(e)] shows a further change and corresponds to that of the transistor structure that has been formed. EBIC confirmed that such a structure was created immediately after the current increase occurred. The time difference between the $I-V$ curves seen in Figs. 6(a) and 6(e) is ~100 ms. This is the structure creation time. The EBIC contrast picture of the transistor structure created (in sample B) during the current increase is presented in Fig. 8(a).

To follow the time dependence of this fast current increase, we inserted an oscilloscope and a triggering circuit in the setup, as described in Sec. II. We performed experiments using a dc voltage (sample D; Table I). When the continuously applied voltage reached a certain critical value, a current spike occurred which lasted ~100 ms. One such spike is shown in Fig. 7. The oscillations observed on the level of 12 mA represent while noise, as is evident from the FFT analysis. The shape of this current–time plot can be explained, assuming that the system shows self-limitation,[7] i.e., as a result of the current increase the cause for its original occurrence is affected and eventually eliminated. This means that significant changes occur in the local electrical properties of the semiconductor during these 100 ms. Indeed, we detected by EBIC the creation of a transistor structure, immediately after the spike, also in this experiment. If after the transistor structure is created [Fig. 8(a)], we continue to apply the high voltage, then this structure increases significantly in size [Fig. 8(b)] during a period of ~1–2 min. This is also evident from the SIMS measurements [see profile 1 in Fig. 3(a)]. The mechanisms of this increase and the self-limitation are considered in Sec. IV.

The high currents that flow during structure creation (Figs. 6 and 7) will lead to large current densities because of the small area of the point contact; therefore, the temperature in the semiconductor can increase locally around this contact. Estimation of this temperature helps explain the time

Downloaded¬23¬Oct¬2002¬to¬132.72.138.3.¬Redistribution¬subject¬to¬AIP¬license¬or¬copyright,¬see¬http://ojps.aip.org/japo/japcr.jsp

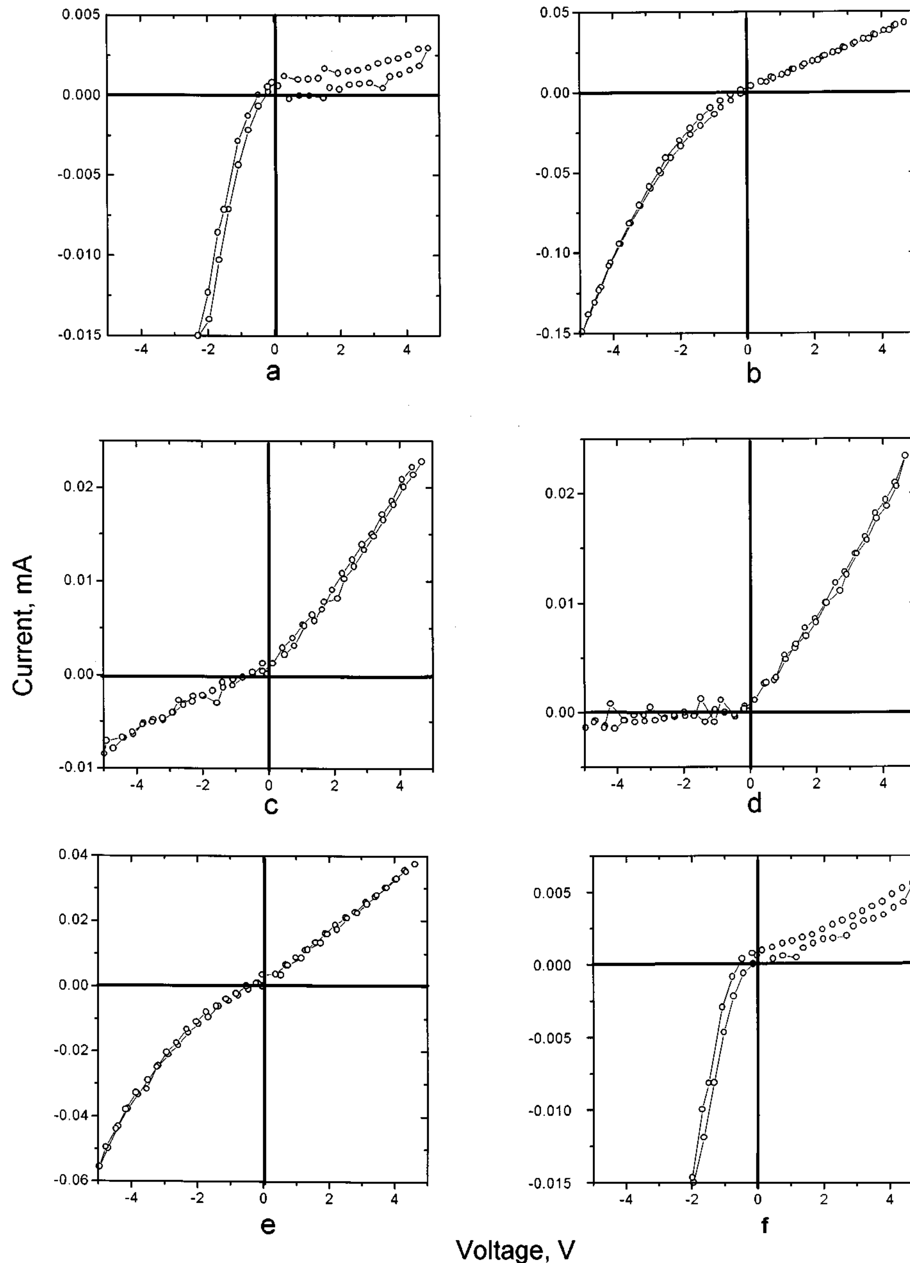

FIG. 5. Contact $I-V$ measurements taken across the transistor structure for which data are shown in Figs. 3(a) and 4 (sample B): (a) Contact on the center of the structure [Fig. 2(b)]; (b)–(c) contacts between center and p region; (d) contact on the p region of the structure; (e) contact between p region and periphery (bulk) of the structure [Fig. 2(b)]; (f) contact on bulk of the sample (n region).

scale of the process and the stability of structures at room temperature after their creation.

D. Temperature estimate during the process of structure formation

The peak power that is dissipated during structure creation, when using periodic voltage application [Fig. 1(b)], varies from ~1.5 to ~3 W. This is ~2–5 times more than the power dissipated during steady state, before and after the current surge. To estimate the temperatures corresponding to this range of dissipated power, we used a method described earlier for $CuInSe_2$,[8] i.e., we measured the power needed to melt contacts of metals with different melting points. Contacts of Zn, Pb, Sn, and In, 50 μm diameter and 20–30 nm thick, were evaporated on the top surface of sample A. A periodic external voltage was applied to these contacts in the reverse direction for a few minutes. Then voltage application was stopped and the contacts were investigated in the SEM at high magnification. In this way the total power, dissipated around the contacts and required for the beginning of their melting, was determined. Figure 9 presents the empirical dependence of the contact temperature on the total power dissipated around the contacts. Because of the large thermal diffusion length in Si (~800 μm at 45 Hz) there is no significant difference in terms of temperature increase between the 10-μm-diam spherical point contact and a 50-μm-diam

Downloaded¬23¬Oct¬2002¬to¬132.72.138.3.¬Redistribution¬subject¬to¬AIP¬license¬or¬copyright,¬see¬http://ojps.aip.org/japo/japcr.jsp

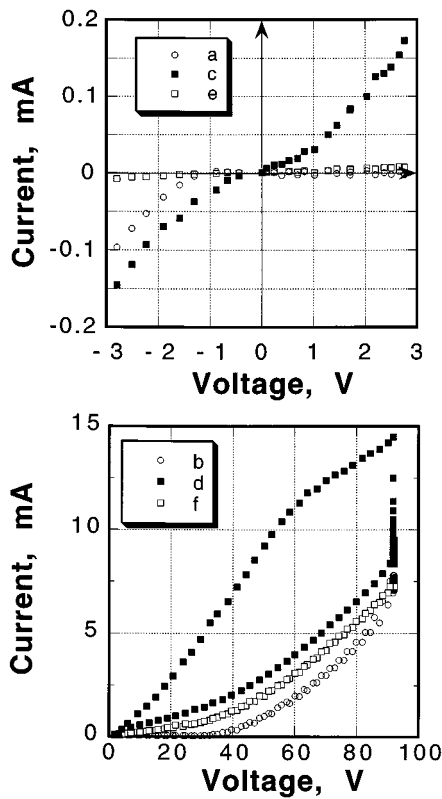

FIG. 6. Typical $I-V$ curves of a W needle/Si:Li/back-contact structure, taken before, during, and after E-field-induced changes of the electrical properties of the material. Sample A; frequency of the signal 45 Hz [Fig. 1(b)]. (a),(c),(e) Low-voltage $I-V$ curves before, during and after changes, respectively; (b),(d),(f) corresponding high-voltage $I-V$ curves before, during, and after changes, respectively.

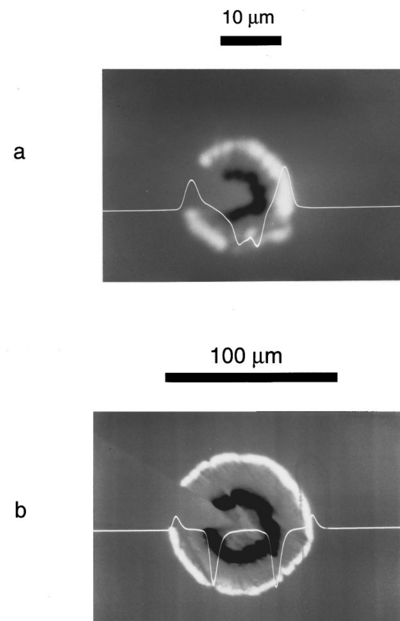

FIG. 8. (a) EBIC contrast picture and superimposed line scan of a transistor created during ~100 ms in sample B. EBIC conditions: accelerating voltage 5 kV; electron-beam spot size: 500 nm. (b) EBIC contrast picture and superimposed line scan of the same structure after high-voltage application was continued for ~2 min. The SIMS profile measured through the center of this structure is presented in Fig. 3(a), profile 1. EBIC conditions: accelerating voltage: 4 kV; electron-beam spot size: 500 nm.

metal contact, evaporated on the surface of Si. From the empirical curve presented in Fig. 9 we estimate that the temperature can reach ~370–450 °C, around a contact, during structure formation.

The above-mentioned temperature estimation can be checked by calculating the temperature increase due to Joule heating in the case of current passing through a spherical point contact. When a voltage is applied periodically to such a contact, the increase in temperature ΔT is given by[17]

$$\Delta T=\frac{0.5P}{\pi K_{\mathrm{th}}R_0}, \tag{1}$$

where P is the average power dissipated around the contact, R_0 is the spherical contact radius, and K_{th} the thermal conductivity of the material. The average dissipated power is $(IV)/3$, where I is the amplitude of current through the con-

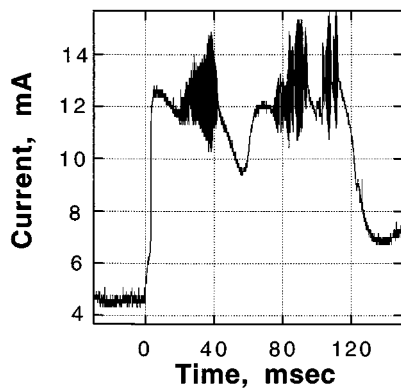

FIG. 7. Time dependence of current through the structure during electric-field-induced changes of the electrical properties of sample D. dc voltage was applied to the sample. Triggering occurred at 0 ms.

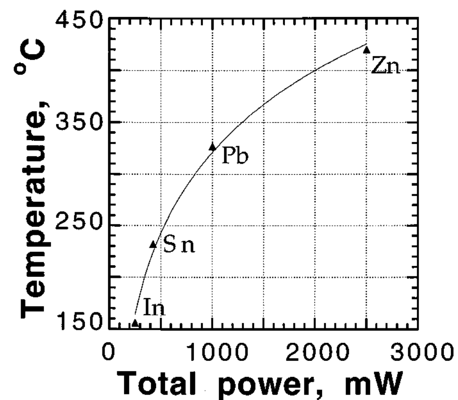

FIG. 9. Empirical dependence of the temperature created around the top contact on the total power dissipated around it (sample A), from observation of melting of contacts of different metals in the SEM. A periodic voltage was applied at 45 Hz. At this frequency the thermal diffusion lengths are such that the temperature increase over the metal contact is essentially uniform ~50 μm into the Si.

Downloaded¬23¬Oct¬2002¬to¬132.72.138.3.¬Redistribution¬subject¬to¬AIP¬license¬or¬copyright,¬see¬http://ojps.aip.org/japo/japcr.jsp

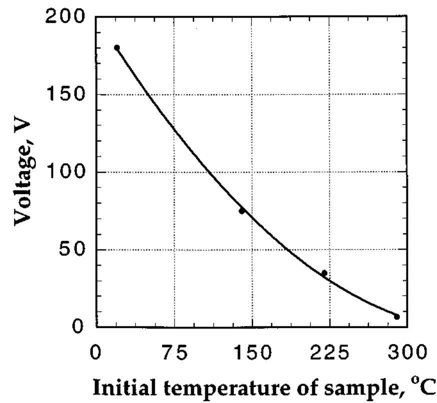

FIG. 10. Dependence of periodic high voltage [Fig. 1(b)] required for structure creation, on the initial global temperature of the sample (sample D).

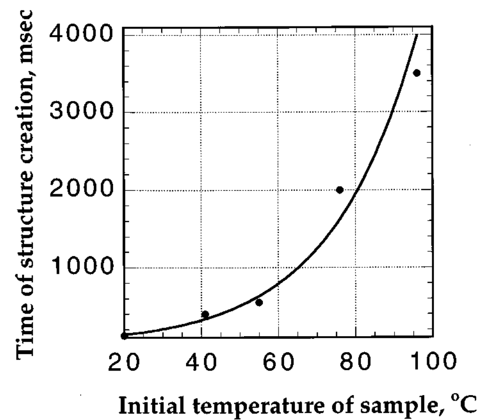

FIG. 11. Dependence of the time of fast structure creation on the initial global temperature of the sample (sample D).

tact and V is the amplitude of voltage applied to this contact. The factor of 1/3 represents the duty cycle of the high-voltage application [Fig. 1(b)]. The semiconductor is assumed to act as an active load. If this is not so, the average dissipated power will be smaller than $(IV)/3$. The average tip radius of a tungsten needle used for voltage application is $R_0=5$ μm. Using $K_{th}=1.31$ W/cm °C, $V=200$ V and $I=15$ mA (current and voltage during structure creation in sample B), we obtain $\Delta T \sim 250$ °C ($T=270$ °C). This value depends strongly on R_0. If, for instance, $R_0=3$ μm then $\Delta T \sim 405$ °C ($T=425$ °C).

E. System near equilibrium

We have seen that initial structure creation takes place in ~100 ms and that it is accompanied by a steep increase of current. This increase occurs when the applied voltage exceeds a certain threshold value. We relate this threshold voltage to the minimum voltage that is needed to reach avalanche conditions (see discussion below). If this is so then this threshold voltage should depend on the global temperature of the sample before external voltage application.[14] To investigate this, sample D was heated *in situ* in the SEM and device structures were created at different temperatures. The dependence of the minimum (periodic) voltage that is required for structure creation on the sample's initial global temperature (before voltage application) is presented in Fig. 10. This shows that the higher this initial global temperature is, the lower the voltage needed for structure creation. The sudden current increase also decreases from values as high as 15 mA, when the bulk of the sample is at ambient temperature (before an external voltage is applied), to ~2 mA, when the bulk of the sample is initially at 80 °C. The time needed for fast structure creation (time of spike, Fig. 7) is longer the higher the initial global temperature of the sample. When the initial global temperature is sufficiently high (>100 °C), fast structure creation, during the spike of current, is not observed. The dependence of the time of fast structure creation on the initial global temperature of the sample is presented in Fig. 11.

All factors mentioned above indicate that when the sample's initial global temperature increases, the system approaches equilibrium and starts to behave as in classical ion migration.[2]

F. Structure stability

The structures that result after voltage application to Si:Li are found to be stable for at least 13 months after their creation, when kept at room temperature. This was reliably checked on a scale of better than 5 μm by EBIC measurements at high magnification. However, annealing the structure at 270 °C for ~20 min leads to a significant decrease in its size, as detected by EBIC. This agrees well with the diffusion coefficient of Li (~10^{-9} cm^2/s) at this temperature.[1]

G. Device action

As for $CuInSe_2$, we find that the transistor structures that are created electroluminesce, emitting near-infrared radiation.[18] Electroluminescence was observed from the n^+-p junction when it was biased in forward direction.[9] Phototransistor action was observed as well.[9] Figure 12 presents transistor action from the structure obtained in sample A. The $I-V$ characteristics were taken *in situ* in the SEM as described in Sec. II. When the electron beam [used to excite the base region; Fig. 2(b)] hits closer to the n^+-p junction, amplification behavior is observed in the first quadrant (Fig. 12). When a region, closer to the (outer) p-n junction is excited, amplification is observed in the third quadrant. The amplification coefficient β can be calculated according to the following formula:[5,9]

$$\beta=\frac{\Delta I_{CE}}{\Delta I_B G}, \qquad (2)$$

where ΔI_{CE} is the change of the current I_{CE}, between top and back contacts (collector and emitter) caused by a change ΔI_B in absorbed beam current I_B (the number of electrons per second deposited in the sample by the electron beam). V_{CE} is the voltage applied between the top and bottom contacts. Positive V_{CE} corresponds to negative top contact and positive

Downloaded¬23¬Oct¬2002¬to¬132.72.138.3.¬Redistribution¬subject¬to¬AIP¬license¬or¬copyright,¬see¬http://ojps.aip.org/japo/japcr.jsp

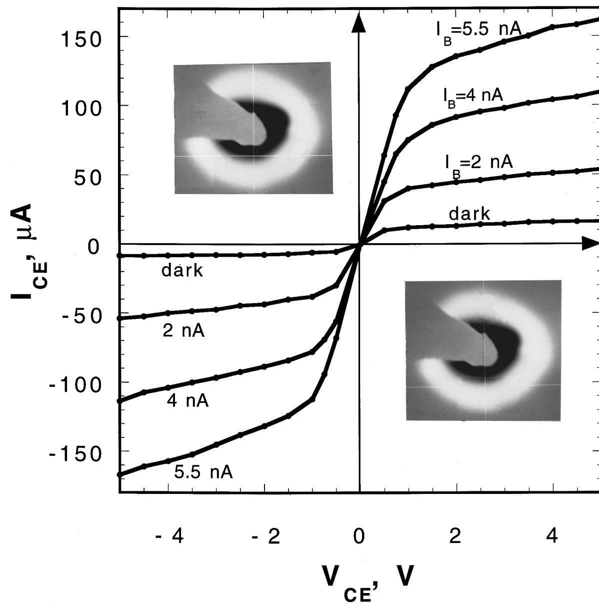

FIG. 12. Dependence of $I-V$ characteristics on location of excitation. Two sets of $I-V$ characteristics and planar EBIC images (inserts) are shown for a transistor structure created in sample A. I_{CE} is current through the structure; V_{CE} is the voltage applied between the top and bottom contacts; I_B corresponds to that part of the electron-beam current that was absorbed in the material. EBIC conditions were the same as for Fig. 2(a). Top: Amplification in the first quadrant: top contact positive. Top insert: planar EBIC contrast of the transistor structure with corresponding position of the electron beam indicated by the cross hair. No transistor behavior is seen in the third quadrant. Bottom: Amplification in the third quadrant: top contact negative. Bottom insert: planar EBIC contrast of the transistor structure with corresponding position of the electron beam indicated by the cross hair. No transistor structure is seen in the first quadrant.

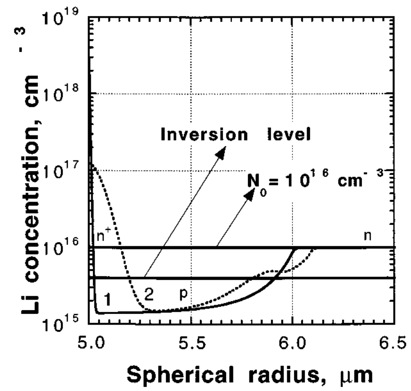

FIG. 13. Calculated redistribution of mobile ions under the influence of electric field. Numerical calculations were performed by a sweeping technique. The horizontal lines shown in this figure present the homogeneous distribution of mobile ions at time 0 (before voltage application) and the level of inversion of the conductivity type. Curves 1 and 2 show the redistribution of ions as a result of external voltage application. Curves 1 and 2 correspond to the situations, achieved 4 and 8 ms, respectively, after switching on the external voltage.

bottom contact. Negative V_{CE} corresponds to the opposite situation. G is a generation factor defined as I_{EBIC}/I_B. I_{EBIC} is the current generated in a semiconductor by the electron beam (of the order of μA), and I_B (of the order of nA) is as defined above. The theoretical maximum of G for 30 keV electrons is $3\times10^4/(E_G\times3.3)\approx8000$,[11] where E_G is the width of the forbidden gap for Si [$\sim$1.12 eV (Ref. 20)]. From ΔI_{CE} at $V_{CE}=+4$ V we find $\beta=4$ for the case presented in Fig. 12 (first quadrant).

True phototransistor action can be observed as well. The base of an n^+-p-n structure, created in sample B, was illuminated by a He–Ne laser (632.8 nm) whose 10 mW (nominally) beam was focused to a spot of $\sim$5 μm diameter. $I-V$ curves were measured between the top and back contacts [Fig. 2(b)] as a function of illumination intensity. The intensity of the laser beam was controlled by neutral density filters and measured by a laser power meter. $I-V$ measurements showed the structure to function as a transistor. This became especially clear from the observation that the quadrant in which the phototransistor action is observed changed with the locus of excitation, similarly to what is shown in Fig. 12 for electron-beam excitation. Actual amplification was estimated as explained in Ref. 5. An increase in laser-beam intensity by 3% increased the device current by 30%.

The fact that actual device action with transistor amplification is seen in the transistor structures suggests that rather abrupt doping profiles are created. Direct evidence for the creation of these profiles was obtained from the SIMS measurements. To obtain further insight we performed numerical simulations of Li profiles that are obtained after drift in Si under the experimental conditions that prevail during the process.

H. Simulations of electromigration of Li in Si

In performing such numerical simulations we made the following assumptions.

(1) A spherical, 10-μm-diam, rectifying metal–semiconductor contact, corresponding to the experimental case of direct contact of the W needle on the semiconductor, is used.

(2) The temperature in the material near the point contact (initial situation) or, during electromigration, around the reverse-biased n-p junction that results [Fig. 2(b)], is $\sim$400 °C. At this temperature the Li ion diffusion coefficient D will be $\sim2.5\times10^{-8}$ cm²/s.[2] Quite a large region (hemisphere with $\sim$50 μm radius) can be heated relatively homogeneously in Si because of its large thermal diffusion length at the frequencies that are used.[14]

(3) All majority-type impurities are ionized at 400 °C. Therefore, the majority-carrier concentration is equal to $(N_D$-$N_A)$, where N_D and N_A are the concentrations of donors and acceptors, respectively. Before E-field application and, in the bulk, after E-field application, the semiconductor is assumed to be electrically homogeneous n type, with $n=1\times10^{16}$ cm^{-3} and $\mu=150$ cm²/V s, i.e., with a bulk electronic conductivity $\sigma=0.3$ Ω^{-1} cm^{-1} (sample B, Table I).

(4) Two p-n junctions are created during the electromigration of ions/dopants [Fig. 2(b)]. One of these junctions (an n^+-p one) is compensated because the applied voltage across it is in the forward direction. The second (p-n) junction is biased in the reverse direction. The mobility of electrons in the n^+ region, that is created, is assumed to be $\sim$150 cm²/V s (Li doping decreases the mobility of electrons significantly from its level in undoped Si, $\sim$1500 cm²/V s;[20] see

Downloaded¬23¬Oct¬2002¬to¬132.72.138.3.¬Redistribution¬subject¬to¬AIP¬license¬or¬copyright,¬see¬http://ojps.aip.org/japo/japcr.jsp

also Table I). The hole mobility in the p region, that is created, is assumed to be $\sim$150 $cm^2/V\,s$ (again Li doping is assumed to decrease mobility from its $\sim$500 $cm^2/V\,s$ value in our starting material, floating zone p-Si). Even if mobilities of the electrons and holes, used in the calculations, are equal to their values in pure (undoped) Si, Li redistribution will not differ from the one presented in Fig. 13. This is because virtually all of the voltage drop is across the reverse-biased p-n junction, while the mobilities enter only for the calculations in the regions outside that junction. However, in those regions we do need to take into account ion drift, because, as shown in Ref. 7, some 5% of the voltage that is applied across the sample drops there.

(5) For simplicity we assume that the p-n junctions created as a result of ion electromigration, as well as the metal–semiconductor barrier, are abrupt [n^+-p junction is <1 μm thick; p-n junction is $\sim$3–4 μm thick; see Figs. 2(b) and 3]. This thickness should be compared to the one of graded-type junctions that can be created in classical ionic conductors.[21] Therefore, the E field in these junctions/barrier was obtained from the Poisson equation for an abrupt profile, solved on the assumption of 100% depleted space-charge region[14] (the validity of this approximation is discussed in Ref. 7). It is assumed that the current through the semiconductor during transistor structure creation (Figs. 6 and 7) does not significantly affect the space charge.[7]

(6) The level of inversion of conductivity type from n to p (concentration of acceptors) is assumed to be 4×10^{15} cm^{-3} [Fig. 3(a)].

The starting equation for the calculations is a continuity equation,

$$\frac{\partial N}{\partial t} = -\frac{1}{e}\,\mathrm{div}\,\mathbf{j}, \tag{3}$$

where N is the concentration of mobile ions (cm^{-3}), t the time (s), e the charge of electron (C), and $\mathbf{j}$ the vector density of the ionic current (A/cm^2).

Rewriting Eq. (3) in spherical coordinates for the case of drift and diffusion, the following second-order partial differential equation for ion electromigration is obtained:

$$\frac{\partial N}{\partial t} = D\,\frac{\partial^2 N}{\partial R^2} + \left(\frac{2D}{R} - \mu_E\right)\frac{\partial N}{\partial R} - \left(\mu\,\frac{\partial E}{\partial R} + \frac{2}{R}\,\mu_E\right)N, \tag{4}$$

where D is the diffusivity of mobile Li ions in Si, E the strength of electric field, and R the spherical coordinate, which varies from R_0=5 μm (radius of the spherical point contact) to R_{FINAL}, the final point of the calculation, where an external electric field does not affect the initial concentration of mobile ions anymore.

The distribution of an electric field in the material outside the space-charge region was obtained from Ohm's law. As was already mentioned, the electric field in the space-charge region of a spherical metal–semiconductor barrier (Schottky barrier) or p-n junction, created by Li electromigration, was obtained from the Poisson equation as is described in Ref. 7 [see also Eq. (8) given below].

We start the calculations considering the situation that results after 4 ms reverse biasing a Schottky contact to a homogeneous n-type semiconductor. The distribution of ions was calculated using Eq. (4). The resulting redistribution of dopants shows the location of the reverse-biased p-n junction that is formed [see Fig. 2(b), junction between bulk n and p region]. We then calculate the effect of the E field on this junction by recalculating the distribution of dopants after another 4 ms. The strength of the electric field in the reverse-biased junction was obtained again from the Poisson equation, solved in the abrupt junction approximation and using the profile of ion distribution obtained after the first 4 ms of voltage application.

Equation (4) was solved by the sweeping technique using the following initial and boundary conditions:

$$N|_{R_0} = N_0 \quad \text{at } t=0, \tag{5}$$

$$N|_{R_{\mathrm{final}}} = N_0 \quad \text{at different } t, \tag{6}$$

$$\mu N_{\mathrm{E}} = D_{\mathrm{chem}}\,\frac{\partial N}{\partial R} \quad \text{at } R=R_0, \tag{7}$$

where N_0 ($\sim10^{16}$ cm^{-3}) is the concentration of mobile ions in the initially homogeneous semiconductor. Boundary condition (7) takes into account that at $R=R_0$ the ionic current is zero, due to the ionic blocking behavior of the point contact. The results of the calculations for two different durations of external voltage application are given in Fig. 13. In the simulations of Li electromigration the occurrence of Li–B pairing is not taken into account (see Sec. IV below). All Li is assumed to be mobile. The results of the simulations resemble the experimental SIMS profiles in terms of the shape of profiles and the magnitude of Li redistribution. The large concentration gradient of Li on the border between Li-rich and -poor regions determines the diffusion flux of Li in the direction opposite to that of the Li drift. This explains a decrease of Li concentration in the Li-rich (n^+) region near the surface and its increase in the Li-poor (p) region in profile 2 with respect to profile 1 (Fig. 13).

IV. DISCUSSION

Based on our earlier work with $CuInSe_2$ we argue that the results presented here can be understood in terms of thermally assisted Coulombic electromigration of Li in Si. A schematic explanation of the present understanding of the process of E-field-induced device structure creation is shown in Fig. 14. We now show how such a scheme fits our observations for the Si:Li system.

As a first step we need to understand the kinetics of structure creation and the mechanism of type conversion. The kinetics of the process are determined by the velocity of Li ions in Si. To calculate this velocity, the strength of the electric field achieved during external voltage application must be estimated. This helps to described the initial steps of the process. Evolution of the structure then leads to type conversion. In Si:Li this is related to the interaction between acceptors (boron) and donors (lithium) which are simultaneously present in our samples. We discuss each of these issues in turn.

Downloaded¬23¬Oct¬2002¬to¬132.72.138.3.¬Redistribution¬subject¬to¬AIP¬license¬or¬copyright,¬see¬http://ojps.aip.org/japo/japcr.jsp

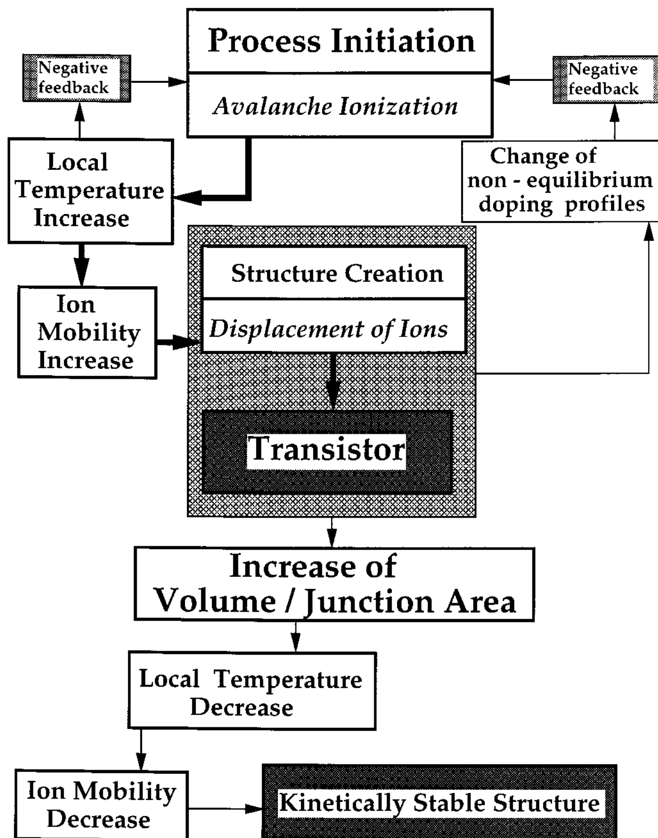

FIG. 14. Schematic explanation of the phenomenon of E-field-induced changes in doping profiles.

A. Estimation of the electric field

The electric field, achieved during the initial stages of structure creation, can be estimated from the Poisson equation written for the space-charge region of a spherical point contact (Schottky barrier),[7]

$$E=\frac{e(N_A-N_D)}{3\epsilon\epsilon_0}\frac{R_S^3-R^3}{R^2}, \tag{8}$$

where R_S is the calculated width of this barrier, ϵ the dielectric constant of the semiconductor, ϵ_0 the permittivity in vacuum, and R varies from R_0 to R_S.

The external voltage applied to the point contact between a needle and the top surface of sample B is, on the average, 150 V. With such a voltage the width of the space-charge region of the metal–semiconductor Schottky barrier is $\sim 3.8\ \mu$m, for a semiconductor with a doping level of $\sim 1\times 10^{16}\ \text{cm}^{-3}$. This yields $R_S=8.8\ \mu$m, because $R_0=5\ \mu$m. Using these numbers, a value of $\sim 10^6$ V/cm is obtained from Eq. (8) for the strength E of the electric field. This value fits that of the electric field in an amorphous Si p-i-n diode, as reported in Ref. 22. Comparable electric field magnitudes were calculated and estimated by us for $CuInSe_2$.[7] These values can be compared to a value of $\sim 5\times 10^5$ V/cm that was reported for a device structure created in ZnSe.[23]

In this estimate of the electric field, as well as in the simulations (Fig. 13), the depletion approximation was used, i.e., all impurities in the space-charge region are ionized. Carrier injection, due to the current spike which takes place during structure creation, does not significantly change the depletion approximation. This was considered by us in detail in Ref. 7.

B. Process initiation

Because of the high electric field created during external voltage application, avalanche conditions are achieved. Electric-field strengths needed to reach the threshold voltage for avalanche ionization can be calculated to be in the range from 5×10^5 to 10^6 V/cm.[20] We ascribe the abrupt increase of current that is observed (Fig. 7) to this ionization. The series of white oscillations seen during the current transient (Fig. 7) may well be related to the system switching in and out of avalanche conditions. This can occur because of negative feedback, one of the causes for which will be considered now. Further work is needed to clarify the nature of these high-frequency oscillations and to determine their relation to the negative feedback.

In the initial stage of the process most of the applied voltage drops across the space-charge region of the reverse-biased metal–semiconductor Schottky barrier [Fig. 2(b)]. The high current [Fig. 6(d)], which passes through this reverse-biased barrier, leads to Joule (IV) heating in the space-charge region of the barrier and around it. Because of this local increase in temperature, Li ion mobility increases in the heated region and the ions, located in this space-charge region, can now move toward the negative W needle under the influence of the E-field [Fig. 2(b)]. The maximum velocity of Li ions can be estimated as

$$v_{\text{Li}}=\mu E=4.1\times 10^{-7}\times 10^6=0.41\ \text{cm/s}.$$

Here μ is calculated from the Nernst–Einstein relation, using a diffusivity of $2.5\times 10^{-8}\ \text{cm}^2$/s. This velocity, taken together with the dimensions of the structure, fits the experimentally observed order of magnitude of the time for initial structure creation, ~100 ms (Figs. 6 and 7). When the current reaches its maximum (Fig. 7), the local temperature increase limits further avalanche ionization by negative feedback (Fig. 14). This is one of the reasons for the self-limiting character of the process. The physical cause for such a negative feedback is a decrease in the mean free path of the electronic carriers. The negative feedback leads to a decrease of current seen in Fig. 7. When the current decreases, the system cools and conditions for the occurrence of avalanche are met again. This explains the second increase of the current. The same negative feedback then leads to a further decrease in current (we explain below the cause for the ultimate decrease of the current to its stationary value).

The negative feedback also explains the decrease of the amplitude of the current spikes and the increase of their duration, i.e., the time for fast structure creation, with the increase of the sample's initial global temperature (Figs. 10 and 11). When, for instance, the initial global temperature of sample Q is ~80 °C, the voltage, required for fast structure creation, is ~110 V (Fig. 10) and the amplitude of the current spike is ~2 mA. The local temperature increase created under a W needle, due to dissipation of ~220 mW (110

Downloaded¬23¬Oct¬2002¬to¬132.72.138.3.¬Redistribution¬subject¬to¬AIP¬license¬or¬copyright,¬see¬http://ojps.aip.org/japo/japcr.jsp

V×2 mA), is ~130 °C (Fig. 9), so that the local temperature will be ~210 °C. The mobility of Li ions corresponding to this temperature is $\sim 10^{-9}$ cm^2/V s and their maximum velocity is $\sim 10^{-3}$ cm/s (compared to 0.4 cm/s velocity when the sample is not heated globally). This difference of more than two orders of magnitude for the velocities of Li ions at the above-mentioned temperatures explains the increase of the time of structure creation, found experimentally (Fig. 11).

As is evident from the simulations of Li electromigration, the concentration of holes in the p region decreases slightly during the evolution of the process (Fig. 13, curve 2 vs 1). Also the part of curve 2 that corresponds to the p region is narrower than that in curve 1.

This is in contrast to the simulations of Cu electromigration in originally electrically homogeneous p-$CuInSe_2$.[7] There the opposite tendency dominates: Cu donor concentration (electron concentration) in the region with converted conductivity type (n-type) increases during the evolution of the process and that region widens. Such an enhancement of the created nonequilibrium profile during the evolution of the process is explained by positive feedback.[7] Apparently in Si:Li, the fluxes determined by Li concentration gradients on the borders between n^+- and p-region and between the p and n (bulk) region (Fig. 13) are comparable with Li ion drift and, therefore, the positive feedback cannot occur.

In Si:Li the changes in carrier concentration p (or N_A-N_D), and the narrowing of the p-region, during the evolution of the process (Fig. 13, curves 1 and 2), lead to a decrease of $\Delta V_{\text{avalanche}}$, the threshold voltage for avalanche multiplication, and of $\Delta V_{p\text{-}n}$, the voltage drop across the reverse-biased p-n (bulk semiconductor) junction [Fig. 2(b)]. Estimations show that $\Delta V_{p\text{-}n}$ decreases ~2 times during the evolution of profile 1 into profile 2 (Fig. 13).[24] At the same time, $\Delta V_{\text{avalanche}}$ decreases 1.75 times.[24] Because initially $\Delta V_{p\text{-}n}$ was very close to $\Delta V_{\text{avalanche}}$, such a decrease leads to $\Delta V_{p\text{-}n} < \Delta V_{\text{avalanche}}$. Therefore, the time course of the process is determined also by the voltage redistribution between the reverse-biased p-n junction and the bulk of the semiconductor. This is the other reason for self-limitation.

For $CuInSe_2$, during the evolution of the process, the electric field needed for avalanche ionization $E_{\text{avalanche}}$ increases ~10 times. The real E field in the junction region decreases by a factor of 2.3 (due to the broadening of the region with the inverted conductivity type). Therefore, in the end the E field is more than one order of magnitude smaller than $E_{\text{avalanche}}$ in $CuInSe_2$.[24] This leads to a suppression of avalanche ionization.

C. Li–B pairing

Before considering further the evolution of the process, the occurrence and consequences of pairing between Li (donor) and B (acceptor) have to be considered. The nature (Coulombic interaction) and the mechanism of this pairing at different temperatures has been treated in detail.[3,25] Direct Coulombic interaction between B^- and Li^+ dominates below ~300 °C. This leads to formation of a $\{Li^+B^-\}$ complex. At higher temperatures Li may substitute for Si in the lattice, due to the formation of Si vacancies, and bind covalently with B, creating a $\{LiB^-\}$ complex. The $\{Li^+B^-\}$ complexes dissociate at these higher temperatures. Estimates made on the basis of the theory given in Ref. 3 show that at 400 °C (the temperature achieved during the ms stage of the process) the ratio $\{Li^+B^-\}/N_A$ is between 10% and 50%. The quantity of mobile Li ions will be determined by the difference between the total amount of Li in the sample (N_D) and the amount of $\{Li^+B^-\}$ and $\{LiB^-\}$ complexes.

This explains why in the SIMS profiles measured in the centers of the transistor structures the decrease of Li concentration [Li] is determined by the B concentration, [B], [Li] ($\sim 2\times 10^{15}$ and $\sim 6.5\times 10^{16}$ cm^{-3}) for profiles 1 of Figs. 3(a) and 3(b), respectively. In our case all the investigated samples are n type (Table I), therefore, [Li]>[B]. If all B is bound with Li, and the electric field is able to make a Li-deficient region from which all mobile Li ions are removed, then, ideally, a region of intrinsic conductivity is created. However, due to the dissociation of the complexes, [Li] decreases below the concentration of acceptors (B) in the Li-deficient region. This leads to the creation of an n^+-p-n rather than an n^+-i-n structure. The hole concentration in the Li-deficient region is [B]–[Li]. The specific resistance of the p region is relatively high because of the small difference between [B] and [Li] in this region. [Li] in the Li-deficient region is slightly lower than [B] in the sample.

To check whether Li–B pairing is relevant in our case, a sample of p-Si with $[B]=6.5\times 10^{16}$ cm^{-3} was doped with Li at 200 °C for ~21 h. Type conversion from p to n did not take place under these conditions. [Li] detected in this sample by SIMS is at the level of $\sim 4.5\times 10^{16}$ cm^{-3}. Reverse bias application up to 200 V to the rectifying metal–semiconductor point contact does not lead to transistor structure creation. This experimental observation proves that under the experimental conditions (applied voltage and current) that are used for structure creation (Table I), Li ions are bound to B ions and, therefore, the excess Li with respect to B ([Li]–[B]) determines the concentration of mobile Li ions.

D. Evolution of the process

The homogeneity of Li distribution is disturbed under the needle during the initiation of the process, as shown in Fig. 2(b). Collection of Li donors under the needle makes this region n^+. Therefore, the rectifying contact between the W needle and the top surface of Si becomes ohmic rather than remaining rectifying (metal contact to n^+ region; see Ref. 7). Then most of the voltage drop will take place around the reverse biased p-n junction [Fig. 2(b)] and this will be the region in which Joule heating is concentrated. The Li ions will thus be pushed out of the reverse-biased p-n junction (due to thermally assisted Coulombic electromigration) creating a p-region deeper in the bulk. In this way, the shallow n^+-p-n structure that is created will propagate into the bulk of the Si and the structure shown in Fig. 8(a) will be created during the following ~100 ms.

In the initial stage of the process, 90%–95% of the applied voltage drops across the space-charge region of the reverse-biased metal–semiconductor Schottky barrier (Ref. 7). The p-region in the n^+-p-n structure that forms is highly resistive, due to the small difference between Li and B con-

Downloaded¬23¬Oct¬2002¬to¬132.72.138.3.¬Redistribution¬subject¬to¬AIP¬license¬or¬copyright,¬see¬http://ojps.aip.org/japo/japcr.jsp

centrations in this region. Therefore, the percentage of voltage which drops inside the reverse-biased p-n junction will decrease due to voltage redistribution between the reverse-biased junction and this high-resistivity p-region.

During propagation of the structure into the bulk of the semiconductor, its volume increases by more than one order of magnitude from the initial value ($\sim 10^{-9}$ cm^{-3}). Therefore, at constant total dissipated power, the temperature will decrease and with it the mobility of ions (Fig. 14). As is mentioned above, the voltage applied to the reverse-biased p-n (bulk of semiconductor) junction during its propagation in the bulk is not able to create avalanche conditions any more. Thus, the increase in affected volume, due to structure formation and the decrease of avalanche multiplication will stop the electromigration of ions. The current that passes through the structure is limited by a reverse-biased p-n junction. This reduces the current to its steady-state value of ~ 7 mA, as is seen in Fig. 7. Further work is needed to prove this mechanism. If confirmed then it should be possible, by way of numerical simulations and time-resolved experiments, to arrive at a quantitative explanation of the current transient.

E. Stability of the structure

The stability of the structures that are created can be understood kinetically. When the external voltage is switched off, the temperature of the semiconductor returns to ambient. The diffusion coefficient of Li ions at room temperature is $\sim 10^{-15}$ cm^2/s.[26] Therefore, 8 years would be required to observe a displacement of Li ions over 5 μm.

F. Comparison of Si:Li and $CuInSe_2$

The main feature which is relevant for both systems is the presence of electrically active species able to migrate at moderate (230–400 °C) temperatures under the influence of a strong electric field. Estimates of this field give in both cases values of 10^5–10^6 V/cm (see present work and Ref. 7). Such a strong electric field creates a regime of avalanche multiplication of electronic carriers and determines the abrupt initiation of the process for both systems.

Mobilities of Li and Cu ions increase by five orders of magnitude relative to room-temperature values, due to the local temperature increase (Refs. 1 and 7). This leads to fast electromigration of ions in the bulk semiconductor. The subsequent temperature decrease that results from the volume increase of the structures leads to the decrease of ion mobility for both systems.

One of the factors which determines the suppression of avalanche multiplication by negative feedback in both systems is the local temperature increase. Other factors are the change of the majority-carrier concentration in the reverse-biased n-p ($p-n$) junctions and the change in the shape of the nonequilibrium ion profiles during their evolution. Both those changes lead to changes of $\Delta V_{\text{avalanche}}$ and of $\Delta V_{p\text{-}n(n\text{-}p)}$. In the case of Si:Li, $\Delta V_{p\text{-}n}$ decreases together with $\Delta V_{\text{avalanche}}$. In the case of $CuInSe_2$, $\Delta V_{n\text{-}p}$ increases together with $\Delta V_{\text{avalanche}}$ ($E_{\text{avalanche}}$);[24] but, in both cases the end result is that $\Delta V_{n\text{-}p(p\text{-}n)} < \Delta V_{\text{avalanche}}$.

Creation of an extended ($\sim$100-μm-diam) transistor structure in $CuInSe_2$ requires 20–100 ms. In Si:Li the process of structure creation is divided into ''fast'' (ms scale) and ''slow'' (up to a few min) stages. This is explained by Li–B pairing in Si:Li and by the redistribution of the applied voltage between the bulk semiconductor and the reverse-biased p-n junction. Contrary to the case of Si:Li, there is no evidence for pairing between mobile donors and immobile acceptors in $CuInSe_2$. This is in agreement with the ease by which the electrical conductivity type can be converted in $CuInSe_2$ (Ref. 7). In Si:Li, type conversion is limited because of Li–acceptor (B) pairing.[25]

The E-field-induced structures are stable at room temperature for at least 1 year for both systems. For Si:Li, published values of diffusivities at 20 °C fit kinetic stabilization of the structures.[26] In the case of $CuInSe_2$, the temperature dependence of Cu diffusion coefficients[27] indicates that its dependence on local composition should be considered, because of suspected E-field-induced changes in defect concentrations.[24]

V. CONCLUSIONS

High-voltage application to n-Si, prepared by homogeneous doping of floating zone p-Si with Li, leads to creation of n^+-p-n structures as shown by SIMS, EBIC, $I-V$, and STM measurements. Actual type conversion is proven by STM $I_{\text{tunnel}}-V$ characteristics. The mechanism that leads to such structure creation is that of thermally assisted Coulombic electromigration of Li ions. SIMS data show that the magnitude of mobile Li redistribution is determined by Li–B pairing in Si. The results obtained extend earlier work of ours on $CuInSe_2$,[5–8] and of, among others, Pell on Si:Li,[2] in which a p-i-n structure was created as the result of reverse biasing a p-n junction created in p-Si by Li in-diffusion.

Further work might well lead to sufficient control over the process, to make *in situ* structure creation in the SEM into a new way for the fabrication of Li-drifted Si detectors. Many μm-sized transistors–detectors could then be created on one Si wafer. This may be of interest for the construction of two-dimensional x-ray detectors. Electric-field-induced device creation at room temperature can thus contribute to technology for microstructure fabrication.

ACKNOWLEDGMENTS

D.C., L.C., and V.L. thank the Israeli Ministry of Science and the Arts, the DG XII of the European Union in the framework of the EU–Israel Research Program, the U.S.–Israel Binational Science Foundation, Jerusalem, Israel, and the Minerva Foundation, each for partial support for this research. They thank O. Stafsudd (UCLA) for Si wafers. V.L. thanks the Israeli Ministry of Immigrant Absorption for partial support.

[1] C. S. Fuller and J. C. Severiens, Phys. Rev. **96**, 21 (1954).
[2] E. M. Pell, J. Appl. Phys. **31**, 291 (1960).
[3] H. Reiss, C. S. Fuller, and F. J. Morin, Bell Syst. Tech. J. **35**, 535 (1956).
[4] T. Miyachi, S. Ohkawa, T. Emura, M. Nishimura, O. Nitoh, K. Takahashi, S. Kitamura, Y. Kim, T. Abe, and H. Matsuzawa, Jpn. J. Appl. Phys. **27**, 307 (1988).

Downloaded¬23¬Oct¬2002¬to¬132.72.138.3.¬Redistribution¬subject¬to¬AIP¬license¬or¬copyright,¬see¬http://ojps.aip.org/japo/japcr.jsp

[5] D. Cahen, J.-M. Gilet, C. Schmitz, L. Chernyak, K. Gartsman, and A. Jakubowicz, Science **258**, 271 (1992).
[6] K. Gartsman, L. Chernyak, J.-M. Gilet, and D. Cahen, Appl. Phys. Lett. **61**, 2428 (1992).
[7] L. Chernyak, K. Gartsman, D. Cahen, and O. M. Stafsudd, J. Phys. Chem. Solids **56**, 1165 (1995); L. Chernyak, A. Jakubowicz, and D. Cahen, Adv. Mater. **7**, 45 (1995).
[8] L. Chernyak, D. Cahen, S. Zhao, and D. Haneman, Appl. Phys. Lett. **65**, 427 (1994).
[9] L. Chernyak, V. Lyakhovitskaya, and D. Cahen, Appl. Phys. Lett. **66**, 709 (1995).
[10] J. T. Walton, N. Derhacobian, Y. K. Wong, and E. E. Haller, Appl. Phys. Lett. **63**, 343 (1993).
[11] H. J. Leamy, J. Appl. Phys. **53**, 51 (1982).
[12] R. Chapman, M. Kellam, S. Goodwin-Johansson, J. Russ, G. E. McGuire, and K. Kjoller, J. Vac. Sci. Technol. B **10**, 502 (1992).
[13] D. K. Schroder, *Semiconductor Material and Device Characterization* (Wiley, New York, 1990).
[14] M. Shur, *Physics of Semiconductor Devices* (Prentice–Hall, Englewood, 1994).
[15] M. Mcellistrem, G. Haase, D. Chen, and R. J. Hamers, **70**, 2471 (1993); M. Weimer, J. Kramer, and J. D. Baldeschwieler, **39**, 5572 (1989).
[16] N. S. McAlpine, P. McConville, D. Haneman, L. Chernyak, and D. Cahen (unpublished).
[17] H. K. Henisch, *Semiconducting Contacts: An Approach to Ideas and Models* (Clarendon, Oxford, 1984).
[18] L. Chernyak, A. Jakubowicz, and D. Cahen, Adv. Mater. **7**, 45 (1995).
[19] D. Haneman, in *CRC Critical Reviews in Solid State and Materials Science* (CRC, Cleveland, OH, 1988), p. 377.
[20] S. M. Sze, *Physics of Semiconductor Devices* (Wiley, New York, 1981).
[21] I. Riess, J. Phys. Chem. Solids **47**, 129 (1986); Phys. Rev. B **35**, 5740 (1987).
[22] J. B. Chevrier and B. Equer, J. Appl. Phys. **76**, 7415 (1994).
[23] M. A. Haase, J. M. DePuydt, and J. E. Potts, Appl. Phys. Lett. **58**, 1173 (1991).
[24] L. Chernyak, Ph.D. thesis, Feinberg Graduate School, Weizmann Institute of Science, 1995.
[25] E. M. Pell, J. Appl. Phys. **31**, 1675 (1960).
[26] A. Zamouche, T. Heiser, and A. Mesli, Appl. Phys. Lett. **66**, 631 (1995).
[27] G. Dagan, T. F. Ciszek, and D. Cahen, J. Phys. Chem. **96**, 11009 (1992); D. Cahen, L. Chernyak, G. Dagan, and A. Jakubowicz, in *Fast Ion Transport in Solids*, edited by B. Scrosati, A. Magistris, C. M. Mari, and G. Mariotto (Kluwer, Dordrecht, 1993), p. 121.

Downloaded¬23¬Oct¬2002¬to¬132.72.138.3.¬Redistribution¬subject¬to¬AIP¬license¬or¬copyright,¬see¬http://ojps.aip.org/japo/japcr.jsp